



## Flexible parylene-film optical waveguide arrays

S. Yamagiwa,<sup>1</sup> M. Ishida,<sup>1,2</sup> and T. Kawano<sup>1</sup>

<sup>1</sup>Department of Electrical and Electronic Information Engineering, Toyohashi University of Technology, Toyohashi 441-8580, Japan

<sup>2</sup>Electronics-Interdisciplinary Research Institute (EIRIS), Toyohashi University of Technology, Toyohashi 441-8580, Japan

(Received 30 April 2015; accepted 8 August 2015; published online 25 August 2015)

Modulation of neuronal activities by light [e.g., laser or light-emitting diode] using optogenetics is a powerful tool for studies on neuronal functions in a brain. Herein, flexible thin-film optical waveguide arrays based on a highly biocompatible material of parylene are reported. Parylene-C and -N thin layers with the different refractive indices form the clad and the core of the waveguide, respectively, and neural recording microelectrodes are integrated to record optical stimuli and electrical recordings simultaneously using the same alignment. Both theoretical and experimental investigations confirm that light intensities of more than 90% can propagate in a bent waveguide with a curvature radius of >5 mm. The proposed flexible thin-film waveguide arrays with microelectrodes can be used for numerous spherical bio-tissues, including brain and spinal cord samples. © 2015 AIP Publishing LLC. [<http://dx.doi.org/10.1063/1.4929402>]

Compared to electrophysiology, optogenetics,<sup>1</sup> which combines optical and genetic methods to allow neuronal activity to be modulated by light, potentially provide a better understanding of neural circuit functions in the brain. To realize optogenetics with a high spatial resolution, microscale light sources integrated with microscale-electrode array devices have been proposed.<sup>2–5</sup> However, stiff material-based conventional optical devices (e.g., glass fiber and silicon) increase the damage in the brain/tissue,<sup>6,7</sup> preventing chronic studies of neurons. Although recent advances in light-emitting diode (LED) processes enable the integration of microscale-LEDs, embedded light source LEDs<sup>3</sup> induce electrical crosstalk/noise during the electrical recording of neuronal activities (~tens of microvolts in an extracellular recording). To further enhance the spatial resolution of conventional optogenetics, microscale optical stimulation and electrical measurement<sup>8</sup> must have the same alignment. In addition to these device requirements, a transparent device substrate would be valuable for device placement on a tissue and future cortical imaging applications.<sup>9</sup>

To address the aforementioned technological challenges of conventional optical devices in optogenetics, the approach reported here is based on waveguide arrays of parylene films. The advantages of fabricating waveguide arrays from a parylene film include (i) flexibility, (ii) high biocompatibility, and (iii) a transparency. Although a parylene film has these features, optical propagation of a curved parylene-film waveguide array has yet to be demonstrated. For optogenetic applications, parylene waveguides can be integrated with an array of microscale electrodes, enabling simultaneous optical and electrical measurements with the same alignment (Fig. 1). In addition, light stimuli-induced noise can be eliminated by placing the light source (e.g., laser, LED) outside of the electrically shielded measurement system. As a step toward future optogenetic applications, herein we develop a fabrication process for a parylene-film waveguide array, discuss the process compatibility with microelectrodes, and clarify the bending and the illumination capabilities by

demonstrating optical propagation in a fabricated device with a curvature radius.

To realize a parylene-based waveguide, parylene-C and -N layers with the different refractive indices (parylene-C: 1.639, -N: 1.661) were selected as the cladding and core, respectively. The optical properties of a bent parylene-film-waveguide with a 6- $\mu\text{m}$ -thick parylene-C clad/6- $\mu\text{m}$ -thick parylene-N core/6- $\mu\text{m}$ -thick parylene-C clad were calculated. The light-intensity attenuation  $\gamma_B$  associated with film bending is expressed as

$$\gamma_B = 10(\log R) \left[ \left( \frac{a+2}{2a} \right) \left( \frac{r}{R\Delta} \right) \right], \quad (1)$$

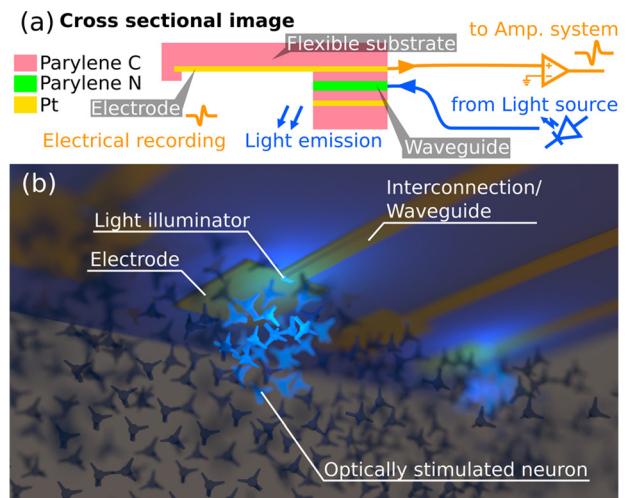


FIG. 1. Schematics of a parylene-film waveguide array with microelectrodes. (a) Cross section of the proposed waveguide device. Parylene-C and -N layers with the different refractive indices (parylene-C: 1.639, -N: 1.661) serve as the clad and the core, respectively. Pt metal layer, which works as the neural recording microelectrode and the light shield, is connected to an amplifier system. (b) Conceptual image of the waveguide array placed on a neuronal tissue showing simultaneous optical stimulation and electrical recording of neurons for optogenetic applications.

where  $r$  is the core radius,  $a$  specifies the shape of the refraction index ( $a=2$  for a parabolic profile,  $a=\infty$  for a step profile),  $R$  is the curvature radius of the bend, and  $\Delta$  is the relative refractive index difference between the core and the cladding.<sup>10</sup> The calculated result shows that more than 50% of the light intensity can propagate in the bent waveguide with a curvature radius of  $>2$  mm (Fig. 2(a)). Additionally, the depth of the evanescent wave is calculated by

$$D_p = \frac{\lambda}{4\pi\sqrt{n_1^2 \sin^2\theta - n_2^2}}, \quad (2)$$

where  $D_p$  is the depth of the evanescent wave,  $\lambda$  is the wavelength,  $n_1$  is the refractive index of the core material,  $n_2$  is the refractive index of cladding material, and  $\theta$  is the angle of the incident. The depth of the evanescent wave is  $<700$  nm for a wavelength of 438 nm, 475 nm, or 580 nm (Fig. 2(b)). These results indicate that the waveguide can be placed on the surface of numerous biological samples with a curvature (e.g., brain and spinal cord) and  $>1$ - $\mu\text{m}$ -thick parylene-C is sufficient as the cladding layer.

A preliminary experiment on the optical propagation in the parylene-film waveguide was executed based on the calculations. The parylene-waveguide was prepared by parylene-based micro electro mechanical system (MEMS) fabrication technology (Fig. 2(c)).<sup>11</sup> First, parylene-C and -N (both 6- $\mu\text{m}$  thick) were deposited on a silicon (Si) substrate as the cladding layer and the core, respectively (Fig. 2(c1)). The core was patterned by oxygen plasma (Fig. 2(c2)) and

then the cladding layer was deposited (Fig. 2(c3)). Finally, the edge of the core was exposed by parylene patterning (Fig. 2(c4)), and the parylene optical waveguide array film was peeled off from the Si substrate (Fig. 2(c5)). The designed width of the core parylene-N was 500  $\mu\text{m}$ , which allows for subsequent coupling with an optical fiber. The length of the core parylene-N was 20 000  $\mu\text{m}$ .

Figs. 2(d) and 2(e) show the fabricated parylene-waveguide array. To confirm light propagation in the individual waveguides, an optical fiber (diameter: 1 mm) connected to a LED was placed on the backside of a waveguide in the array (Fig. 2(d)). The LED emission with a wavelength of 438 nm illuminated the edge of the waveguide (Figs. 2(f) and 2(g)). Although the neuronal experiments with the proposed waveguide arrays will be discussed in the future, the employed wavelength is applicable for optogenetic excitation of neurons.<sup>1</sup>

Fig. 3(a) shows the fabrication process of the parylene-waveguide array embedded in microelectrodes (Fig. 1(a)). First, a sacrificial titanium (Ti) layer ( $\sim 100$  nm) was sputtered on the Si-substrate (Fig. 3(a1)). Next, parylene-C (10  $\mu\text{m}$ ) was deposited as the substrate and then Ti and platinum (Pt) ( $\sim 100$  nm) was sputtered as the light shielding layer (Fig. 3(a2)). Similar to the aforementioned preliminary experiment (Fig. 2(c)), parylene-C (6  $\mu\text{m}$ ) and parylene-N (6  $\mu\text{m}$ ) were deposited as the bottom cladding and core layers, respectively (Fig. 3(a3)) and patterned by oxygen plasma with a mask layer of Ti (Fig. 3(a4)). The Ti mask was removed after patterning. After the deposition and formation

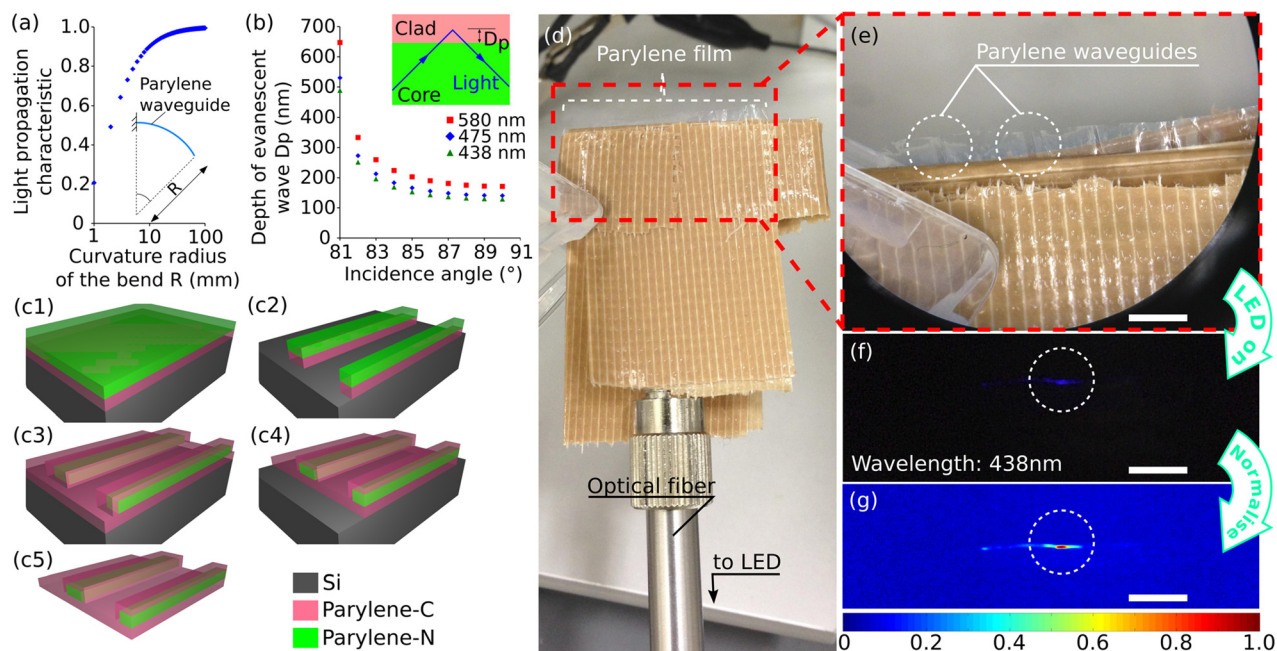


FIG. 2. Calculation and preliminary experimental results of parylene-C(clad)/-N(core)/-C(clad) waveguide. (a) Calculated propagation efficiencies of bent parylene-waveguide with curvature radii from 1 mm to 100 mm. Note that the core parylene-N is 6- $\mu\text{m}$  thick and light attenuation of the waveguide is not considered. (b) Calculated depth of the evanescent wave–incidence angle characteristic of parylene-N(core)/-C(clad) as a function of wavelength (438 nm–580 nm for optogenetic applications). (c) Fabrication process of a parylene-N (core)/-C (clad) waveguide array for the preliminary light propagation tests: depositions of Parylene-C and -N layers on a Si substrate (c1), patterning of parylene-N/-C to form the core (c2), deposition of second parylene-C for the upper cladding layer (c3), patterning of the parylene substrate (c4), and removal of the parylene waveguide array from the Si substrate (c5). (d) Photograph depicting the experimental setup for the preliminary light propagation tests of the fabricated waveguide array. One waveguide in the array is coupled with an optical fiber, which is connected to an LED with the wavelength of 438 nm. (e) Photograph of the tip portion of the parylene-waveguide array. Except for the tip portion, the waveguide array is covered with tape to shield the light. (f) CCD image showing light illumination from the tip section of the coupled waveguide. (g) Normalized light intensity distribution from the CCD image (f). Scale bars in (e), (f), and (g) are 3 mm.

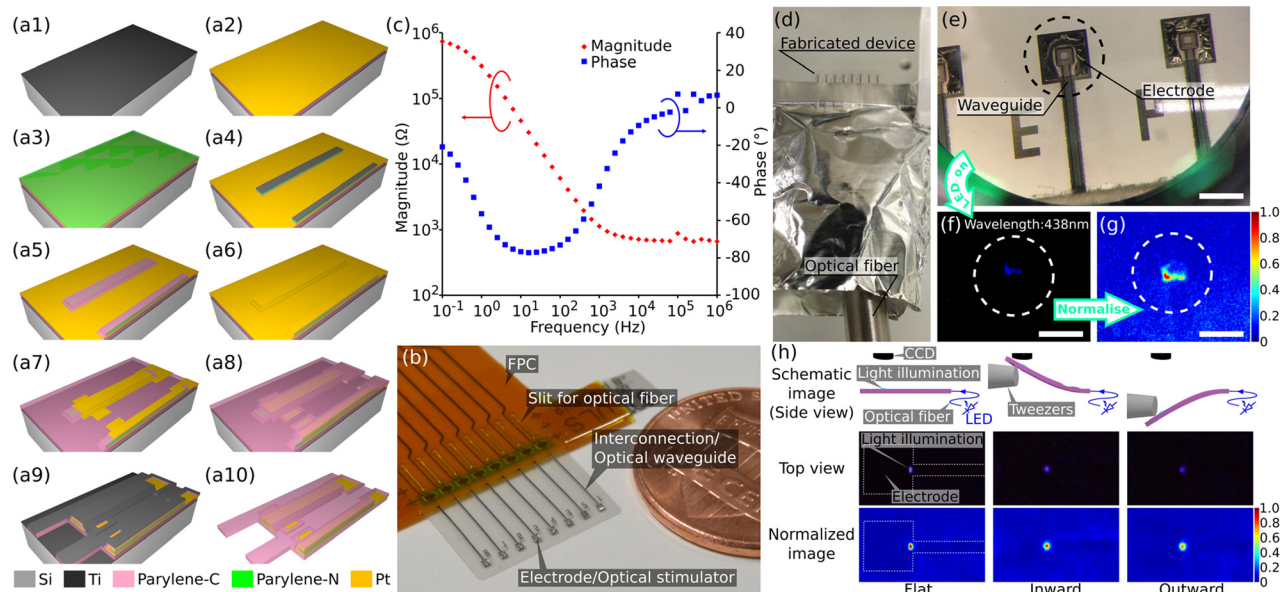


FIG. 3. Fabrication and characterizations of parylene-waveguide array with microelectrodes. (a) Fabrication process of a parylene-waveguide array with microelectrodes: sputtering sacrificial bottom-Ti layer (a1), parylene-C deposition and Pt sputtering (a2), depositions of parylene-C and -N layers and patterning by  $O_2$  plasma with a mask layer of Ti (Ti is removed after patterning) ((a3) and (a4)), deposition and patterning of the second parylene-C layer (a5), sputtering of the second Pt layer and the patterning by RIE ((a6) and (a7)), deposition of the fourth parylene-C layer as the upper insulating layer (a8), patterning of the device substrate of parylene by  $O_2$  plasma with a Ti-mask (a9), and releasing of the parylene waveguide substrate by etching the sacrificial bottom-Ti layer (a10). (b) Photograph of a fabricated waveguide array with a microelectrode packaged with a polymer-based FPC. Film device consists of an array of eight microelectrode/waveguides with a  $1500\text{-}\mu\text{m}$  center-to-center spacing between the waveguides. Each microelectrode is electrically connected via the FPC. Slits embedded in the FPC are designed for subsequent fiber alignments and couplings. US penny is shown for comparison. (c) Magnitude and phase electrical impedance of the Pt-microelectrode measured in room temperature PBS. (d) Photograph of the experimental setup for light propagation tests of the fabricated microelectrode/waveguide array. Similar to Fig. 2(d), one waveguide in the array is coupled with an optical fiber (wavelength of LED = 438 nm). (e) Microscope image of the tip section of the microelectrode/waveguide. CCD image of (f) light illumination from the edge of the waveguide and (g) the normalized light intensity distribution. and (h) demonstration of the light illumination from a bent parylene waveguide. Light was illuminated through the waveguide while the device was bent by tweezers. Scale bars in (e)–(g) are  $500\text{ }\mu\text{m}$ .

of the top parylene-C clad ( $6\text{ }\mu\text{m}$ ) (Fig. 3(a5)), a Pt layer was sputtered and Pt/Ti layer was formed by argon plasma etching as the recording microelectrode ( $500\text{ }\mu\text{m} \times 500\text{ }\mu\text{m}$  for the recording site) and the light shield, respectively (Figs. 3(a6) and 3(a7) and the supplementary material<sup>12</sup>). Then parylene-C ( $10\text{ }\mu\text{m}$ ) was deposited as an insulator (Fig. 3(a8)). Finally, after the hard mask of Ti was sputtered and patterned by  $CF_4$  plasma, the parylene substrate was patterned by oxygen plasma (Fig. 3(a9)), and the device was released from the Si-substrate by Ti sacrificial layer etching with an ammonium solution (Fig. 3(a10)). The designed width of the core parylene-N and the center-to-center spacing between the waveguides were  $70\text{ }\mu\text{m}$  and  $1500\text{ }\mu\text{m}$ , respectively. These parameters were chosen for the subsequent coupling with the optical fiber. There were eight waveguide channels in the array within the  $13\text{ }100\text{ }\mu\text{m}$ -wide parylene substrate. The length of the core was  $10\text{ }000\text{ }\mu\text{m}$ , which is shorter than that of preliminary devices ( $20\text{ }000\text{ }\mu\text{m}$ , Figs. 2(d)–2(g)).

The fabricated device was packaged with a polymer-based flexible-printed-circuit (FPC) (Fig. 3(b)), and the impedance of the microelectrode was measured in a phosphate-buffered saline (PBS) at room temperature (Fig. 3(c)). The measured impedance at  $1\text{ kHz}$  was  $\sim 1.1\text{ k}\Omega$ , which is low enough to record the neural signals, including electrocorticograms (ECoGs) ( $<500\text{ Hz}$ ),<sup>13</sup> intracortical local field potentials (LFPs) ( $<500\text{ Hz}$ ), and action potentials (APs) ( $\sim 1\text{ kHz}$ ).<sup>14</sup> Similar to the preliminary test (Fig. 3(d)), light propagation in the waveguide and illumination through the center of the electrode were observed using the same

LED light source (wavelength = 438 nm) (Figs. 3(d)–3(g)). The intensity of the light stimulation through the waveguide depends on the input power of the light source. From the transmission tests using an input LED power of  $285\text{ mW}$  (Figs. 3(f) and 3(g), the used fiber diameter is  $3\text{ mm}$ ), the intensity per area measured at the edge of the fabricated waveguide is  $1.43\text{ mW/mm}^2$ . Although the mismatches (lateral offset, NA mismatch, angular misalignment, and core diameter mismatch etc.) between the fiber ( $3\text{-mm}$  diameter) and the waveguide ( $6\text{-}\mu\text{m} \times 70\text{-}\mu\text{m}$  cross-sectional area) caused losses in the connection, the measured intensity of the fabricated waveguide is sufficient for light stimuli to neurons in optogenetics [e.g.,  $0.1\text{ mW/mm}^2 - 1\text{ mW/mm}^2$  for channelrhodopsin-2 (ChR2)].<sup>1,15,16</sup> These results indicate that the proposed optical stimulating waveguide and electrical recording microelectrode can be integrated within a flexible parylene thin-film for numerous optogenetic applications.

To confirm the light propagation in the bent waveguide, a bending test on the fabricated microelectrode/waveguide array was conducted. In this experiment, the optical fiber, which was connected to the LED (wavelength = 438 nm), was located on the backside of the fabricated waveguide. Light was illuminated through the waveguide while the device was bent by tweezers (Fig. 3(h) and the supplementary material<sup>12</sup>). To further assess light attenuation associated with bending of the waveguide (Fig. 2(a)), the waveguide was bent by placing the device substrate on a curved jig. In this experiment, three concave jigs with various curvature radii ( $2\text{ mm}$ ,  $5\text{ mm}$ , and  $10\text{ mm}$ ) were prepared by a 3D printer (Replicator 2 $\times$ ,

MakerBot Inc.) (Fig. 4(a), “Schematic image” and “Side view”). The results confirm that the attenuated light illumination is associated with device bending (Fig. 4(a), “LED on” and “Normalized image”). Compared to the curvature radius of infinity (the normalized maximum light intensity was set to 1.00), the normalized intensities at the curvature radii of 2 mm, 5 mm, and 10 mm were 0.282, 0.929, and 1.00, respectively (Fig. 4(b)). The calculated data agrees well with the experimental data (Fig. 2(a)), indicating that the flexible waveguide can be used for numerous biological tissues with sub-ten millimeter curvatures ( $>5$  mm) without significant light attenuation ( $>90\%$  light intensity).

We propose a parylene-film flexible waveguide, which has a light source outside of the measurement system, because this measurement scheme eliminates light stimuli-induced noise (e.g., electrical signals for the light source of laser or LED) (Fig. 1(a)). For the optogenetic applications, an outside light source (e.g., laser, LED)<sup>8</sup> can realize a light intensity sufficient to stimulate neurons ( $> 1 \text{ mW/mm}^2$ )<sup>1,15,16</sup> and provide numerous wavelengths of light stimuli for optogenetic applications without replacing the waveguide device, which is in physical contact with the biological tissue. As demonstrated in the illumination tests, the mismatches between the optical fiber and the fabricated waveguide caused the reduced optical power ( $1.43 \text{ mW/mm}^2$  at the edge of the waveguide), which will be improved by considering the fiber-waveguide connection (e.g., connector/adaptor, mirror,<sup>17</sup> lens,<sup>18</sup> grating,<sup>19</sup> or micro-LED light source integrated with the waveguide).

According to device bending tests, the proposed device is applicable to biological tissues with a sub-ten millimeter curvature without significant light attenuations ( $>90\%$  light intensity for  $>5$  mm curvature radius, Fig. 4(b)). The curvature radii of mouse’s and rat’s brain surfaces in the coronal section are  $\sim 6.0$  mm and  $\sim 9.7$  mm, respectively, which are obtained at 6-mm caudal from each bregma. Since the light intensity can be increased with increase in intensity of the light source, the proposed device can possibly be used for macaque’s spinal cord, which has a curvature radius of  $\sim 3.5$  mm. In the optogenetic applications, the waveguide film enables the conformal wrapping of the tissue, while the tissue is illuminated. Although herein we discuss the bending properties of the waveguide, the proposed device should be applicable to “flat” biological samples, including retina,<sup>5,20</sup> brain slices,<sup>21</sup> and cultured neurons.<sup>15</sup>

In the future, we plan to form the waveguide array into a shank array, which will allow the parylene-waveguides to penetrate into a tissue and illuminate deep layer neurons. Such shank-waveguide arrays can be formed by simply utilizing a shank layout of the parylene-film substrate. These thin-film flexible shank microelectrode/waveguide arrays can penetrate into a tissue by using a releasable structural support.<sup>3</sup> The light-evoked electrical activities of the deep layer neurons can be detected with integrated microelectrodes (Fig. 3(a)), potentially realizing multisite deep-layer optogenetic applications.

The proposed fabrication process allows the integration of microelectrodes composed of not only Pt but also other

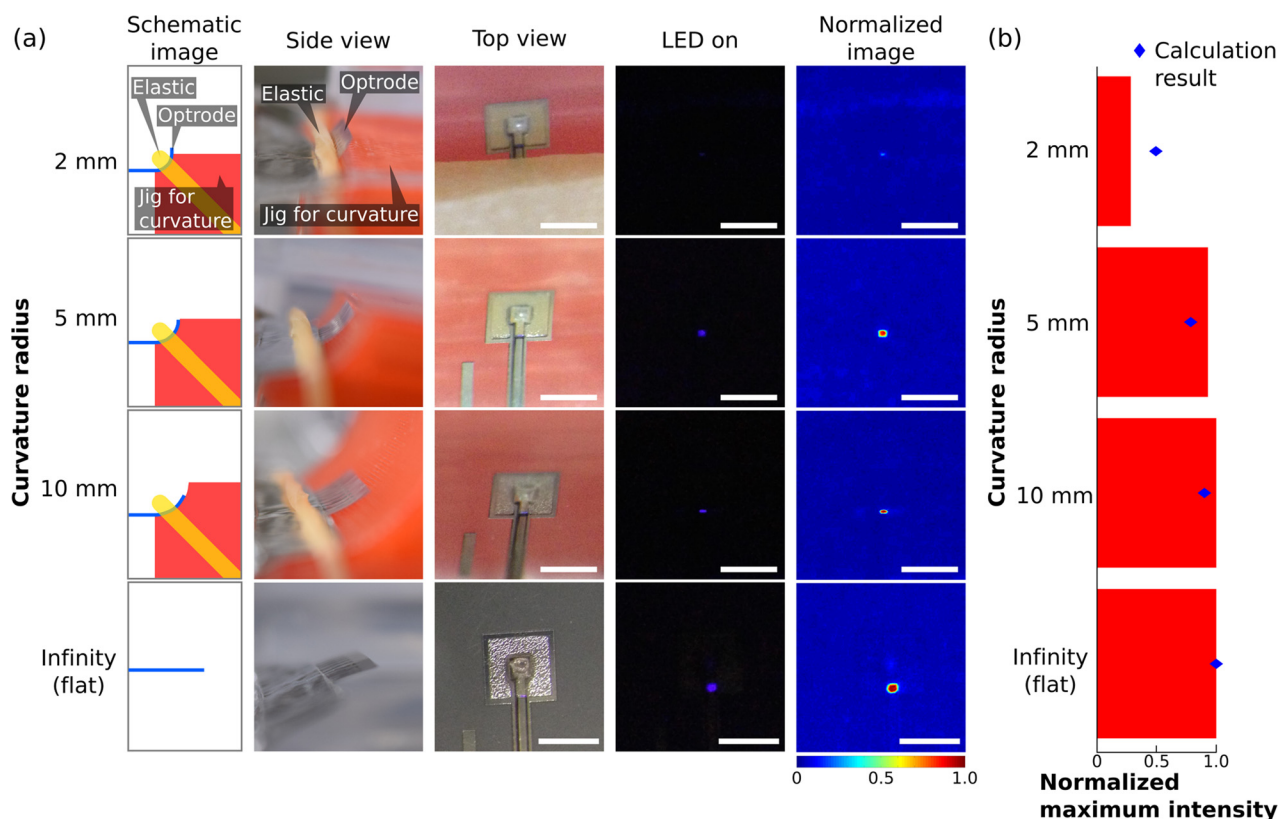


FIG. 4. Experimental results of the light illumination from a bent parylene waveguide. (a) Light illumination from a bent waveguide with various curvature radii of 2 mm–10 mm. Illumination with “flat” waveguide is also tested (right panels). Panels from top to bottom correspond to schematics of the setup, device side-view, device top-view, CCD image while illuminating, and the normalized intensity distribution. (b) Normalized maximum intensity taken from the experimental results [bottom panels in (a)]. Intensity values are 0.282, 0.929, 1.00, and 1.00 for the curvature radius of 2 mm, 5 mm, 10 mm, and infinity (flat), respectively. Theoretical intensity is also graphed. Scale bars in (a) are  $500 \mu\text{m}$ .

materials, depending on the specific device application. An organic material such as poly(3,4-ethylenedioxythiophene) (PEDOT)<sup>22</sup> can be used as the electrode in an all organic material-based device for chronic applications that require a high biocompatibility. In addition, integration of a transparent electrode and interconnection, such as indium tin oxide (ITO),<sup>23,24</sup> PEDOT, and grapheme,<sup>9</sup> can be used for an all transparent material-based device, realizing a powerful tool in simultaneous optogenetic and optical imaging applications.<sup>9</sup>

In summary, a flexible thin-film highly biocompatible waveguide array is fabricated using parylene-based MEMS fabrication technology. Parylene-C and -N with the different refractive indices can serve as the clad and core of the waveguide, respectively, with wavelengths of 438 nm–580 nm for optogenetic applications. Both theoretical calculations and bending tests on prepared waveguides confirm that a light intensity of more than 90% can propagate in a bent waveguide with a curvature radius of >5 mm. This flexible waveguide has potential not only for numerous spherical tissues (e.g., rodent brain and monkey's spinal cord) but also for flat tissues (e.g., retina and brain slices). In addition, the waveguide array can be integrated with microelectrodes, allowing light-evoked neural activities (ECoG, intracortical LFP, and AP) to be simultaneously recorded using the same alignment. These results demonstrate that the proposed parylene-waveguides can be used for optogenetic applications.

In the future, this electrode/waveguide array will be used as a multisite penetrating device into a tissue by forming a shank shape on the parylene-substrate. Compared to the conventional optical devices, this penetrating parylene-film electrode/waveguide array has the high biocompatibility and flexibility, in which properties minimize the device penetration-induced neuronal tissue damage. Because the device features of thin-film flexible multichannel waveguides and a post-silicon process are feasible, this technology has the potential for diverse applications, including optical interconnections for device-to-device communications<sup>25</sup> and optical pressure sensors.<sup>26</sup>

The authors gratefully acknowledge Professor Numano for her help with illumination tests. This work was supported by Grant-in-Aids for Scientific Research (S, A), Young Scientists (A), and the PRESTO Program from JST.

<sup>1</sup>A. M. Aravanis, L. Wang, F. Zhang, L. A. Meltzer, M. Z. Mogri, M. B. Schneider, and K. Deisseroth, "An optical neural interface: *In vivo* control of rodent motor cortex with integrated fiberoptic and optogenetic technology," *J. Neural Eng.* **4**(3), S143 (2007).

<sup>2</sup>I. J. Cho, H. W. Baac, and E. Yoon, "A 16-site neural probe integrated with a waveguide for optical stimulation," *Proc. MEMS* **2010**, 995.

<sup>3</sup>T. Kim, J. G. McCall, Y. H. Jung, X. Huang, E. R. Siuda, Y. Li, J. Song, Y. M. Song, H. A. Pao, R. H. Kim, C. Lu, S. D. Lee, I. S. Song, G. Shin, R. A. Hasani, S. Kim, M. P. Tan, Y. Huang, F. G. Omenetto, J. A. Rogers, and M. R. Bruchas, "Injectable, cellular-scale optoelectronics with applications for wireless optogenetics," *Science*. **340**(6129), 211 (2013).

<sup>4</sup>K. Y. Kwon, B. Sirowatka, A. Weber, and W. Li, "Opto- $\mu$ ECoG Array: A hybrid neural interface with transparent  $\mu$ ECoG electrode array and integrated LEDs for optogenetics," *IEEE T. Biomed. Circ. S.* **7**(5), 593 (2013).

<sup>5</sup>J. Zhang, F. Laiwalla, J. A. Kim, H. Urabe, R. V. Wagenen, Y. K. Song, B. W. Connors, F. Zhang, K. Deisseroth, and A. V. Nurmikko, "Integrated device for optical stimulation and spatiotemporal electrical recording of neural activity in light-sensitized brain tissue," *J. Neural Eng.* **6**(5), 055007 (2009).

<sup>6</sup>D. H. Szarowski, M. D. Andersen, S. Retterer, A. J. Spence, M. Isaacson, H. G. Craighead, J. N. Turner, and W. Shain, "Brain responses to micro-machined silicon devices," *Brain Research* **983**(1–2), 23 (2003).

<sup>7</sup>J. Thelin, H. Jorntell, E. Psouni, M. Garwicz, J. Schouenborg, N. Danielsen, and C. E. Linsmeier, "Implant size and fixation mode strongly influence tissue reactions in the CNS," *PLoS One* **6**(1), e16267 (2011).

<sup>8</sup>M. Sakata, T. Nakamura, T. Matsuo, A. Goryu, M. Ishida, and T. Kawano, "Vertically integrated metal-clad/silicon dioxide-shell microtube arrays for high-spatial-resolution light stimuli in saline," *Appl. Phys. Lett.* **104**, 164101 (2014).

<sup>9</sup>D. W. Park, A. A. Schendel, S. Mikael, S. K. Brodnick, T. J. Richner, J. P. Ness, M. R. Hayat, F. Atry, S. T. Frye, R. Pashaie, S. Thongpang, Z. Ma, and J. C. Williams, "Graphene-based carbon-layered electrode array technology for neural imaging and optogenetic applications," *Nat. Commun* **5**, 5258 (2014).

<sup>10</sup>W. C. Wang, W. R. Ledoux, B. J. Sangeorzan, and P. G. Reinhall, "A shear and plantar pressure sensor based on fiber-optic bend loss," *J. Rehabil. Res. Dev.* **42**(3), 315 (2005).

<sup>11</sup>S. Yamagiwa, M. Ishida, and T. Kawano, "Self-curling and -sticking flexible substrate for ECoG electrode array," *Proc. MEMS* **2013**, 480.

<sup>12</sup>See supplementary material at <http://dx.doi.org/10.1063/1.4929402> for Pt/Ti patterning and movie of light illumination while device bending.

<sup>13</sup>B. Rubehn, C. Bosman, R. Oostenveld, P. Fries, and T. Stieglitz, "A MEMS-based flexible multichannel ECoG-electrode array," *J. Neural Eng.* **6**(3), 036003 (2009).

<sup>14</sup>A. Fujishiro, H. Kaneko, T. Kawashima, M. Ishida, and T. Kawano, "*In vivo* neuronal action potential recordings via three-dimensional microscale needle-electrode arrays," *Sci. Rep.* **4**, 4868 (2014).

<sup>15</sup>N. Grossman, V. Poher, M. S. Grubb, G. T. Kennedy, K. Nikolic, B. McGovern, R. B. Palmini, Z. Gong, E. M. Drakakis, M. A. A. Neil, M. D. Dawson, J. Burrone, and P. Degenaar, "Multi-site optical excitation using ChR2 and micro-LED array," *J. Neural Eng.* **7**(1), 016004 (2010).

<sup>16</sup>Z. Li, J. Liu, M. Zheng, and X. Z. S. Xu, "Encoding of both analog- and digital-like behavioral outputs by one *C. elegans* interneuron," *Cell* **159**(4), 751 (2014).

<sup>17</sup>L. Y. Lin, E. L. Goldstein, and R. W. Tkach, "Free-space micromachined optical switches with submillisecond switching time for large-scale optical crossconnects," *IEEE Photonics Technol. Lett.* **10**(4), 525 (1998).

<sup>18</sup>M. C. Wu, L.-Y. Lin, S.-S. Lee, and K. S. J. Pister, "Micromachined free-space integrated micro-optics," *Sens. Actuators, A-Phys.* **50**(1–2), 127 (1995).

<sup>19</sup>D. Taillaert, F. V. Laere, M. Ayre, W. Bogaerts, D. V. Thourhout, P. Bienstman, and R. Baets, "Grating couplers for coupling between optical fibers and nanophotonic waveguides," *Jpn. J. App. Phys.* **45**(8), 6071 (2006).

<sup>20</sup>T. Harimoto, K. Takei, T. Kawano, A. Ishihara, T. Kawashima, H. Kaneko, M. Ishida, and S. Usui, "Enlarged gold-tipped silicon microprobe arrays and signal compensation for multi-site electroretinogram recordings in the isolated carp retina," *Biosens. Bioelectron.* **26**(5), 2368 (2011).

<sup>21</sup>B. K. Andrasfalvy, B. V. Zemelman, J. Tang, and A. Vaziri, "Two-photon single-cell optogenetic control of neuronal activity by sculpted light," *Proc. Natl. Acad. Sci. U.S.A.* **107**(26), 11981 (2010).

<sup>22</sup>S. F. Cogan, "Neural stimulation and recording electrode," *Annu. Rev. Biomed. Eng.* **10**, 275 (2008).

<sup>23</sup>P. Ledochowitsch, E. Olivero, T. Blanche, and M. M. Maharbiz, "A transparent  $\mu$ ECoG array for simultaneous recording and optogenetic stimulation," *Conf. Proc. IEEE Eng. Med. Biol. Soc.* **2011**, 2937.

<sup>24</sup>O. Marre, D. Anodei, N. Deshmukh, K. Sadeghi, F. Soo, T. E. Holy, and M. J. Berry II, "Mapping a complete neural population in the retina," *J. Neurosci.* **32**(43), 14859 (2012).

<sup>25</sup>H. Ma, A. K.-Y. Jen, and L. R. Dalton, "Polymer-based optical waveguides: Material, processing, and devices," *Adv. Mater.* **19**(14), 1339 (2002).

<sup>26</sup>M. Ramuz, B. C.-K. Tee, J. B.-H. Tok, and Z. Bao, "Transparent, optical, pressure-sensitive artificial skin for large-area stretchable electronics," *Adv. Mater.* **24**(24), 3223 (2012).